Sequencing of Cutaneous Squamous Cell Carcinoma Primary Tumors and Patient-Matched Metastases Reveals *ALK* as a Potential Driver in Metastases and Low Mutational Concordance in Immunocompromised Patients

Marissa B. Lobl[1], Dillon D. Clarey[1], Shauna Higgins[2], Adam Sutton[1,3] and Ashley Wysong[1,2,3]

Cutaneous squamous cell carcinoma is a common skin cancer that is responsible for 1,000,000 cases and up to 9,000 deaths annually in the United States. Metastases occur in 2−5% of patients and are responsible for significant morbidity and mortality. The objective of this study is to perform targeted next-generation sequencing on a cohort of squamous cell carcinoma primary tumors and patient-matched lymph node metastases. An oncology 76-gene panel was run from formalin-fixed paraffin-embedded samples of patient-matched primary squamous cell carcinomas (10) and resultant metastases (10). *ALK* was discovered to be a driver mutation in metastases using two different algorithms, oncoCLUSTand dNdScv. Mutational concordance between primary tumors and metastases was notably lower in immunosuppressed patients, especially among pathogenic mutations (41.7% vs. 83.3%, $P = 0.01$). Sequencing of matched squamous cell carcinoma primary tumors and lymph node metastases identified genes and pathways that may have clinical importance, most notably *ALK* as a potential driver mutation of metastasis. Sequencing of both primary tumors and metastases may improve the efficacy of targeted therapies.

JID Innovations (2022);**2:**100122 doi:10.1016/j.xjidi.2022.100122

INTRODUCTION

Cutaneous squamous cell carcinoma (SCC) is the second most common skin cancer, with 1,000,000 cases and up to 9,000 deaths annually in the United States (American Cancer Society, 2018; Karia et al., 2013; Mansouri and Housewright, 2017; Rogers et al., 2015). Although a majority of SCCs remain localized, approximately 2−5% of tumors metastasize (Brougham et al., 2012; Joseph et al., 1992). Organ-transplant recipients are especially susceptible to developing SCC and have a risk of 65−100 times than that of the general population (Lindelöf et al., 2000). In addition, organ-transplant recipients generally have a higher risk of metastasis, estimated at 7.3−11.0% (Genders et al., 2019). Metastasis and local invasion are responsible for significant patient morbidity and mortality in SCC (Bernal Martínez et al., 2020). Because therapeutic options for advanced and metastatic SCC are currently limited, studying mutations specific to metastatic SCC may lead to improved and targeted treatments.

The literature describing genetic mutations in metastases arising from SCC is relatively sparse. However, several recent studies have begun to characterize these mutations. Li et al. (2015) performed targeted sequencing on 504 cancer-associated genes on 29 lymph node metastases arising from SCC. Results showed that C>T mutations were the dominant substitution, and *TP53*, *CDKN2A*, and *NOTCH1* were altered in over 50% of samples (Li et al., 2015). A study by Al-Rohil et al. (2016) also performed targeted sequencing on 11 lymph node metastases arising from SCCs and found many mutations in *TP53*, *TERT*, *NOTCH1*, *ASXL1*, *CREBBP*, *LRP1B*, and *MLL2* (Al-Rohil et al., 2016). These studies provide useful information on gene mutations seen in metastases; however, the mutations that are conserved or altered from metastatic primary tumors to metastases are yet to be discovered. To our knowledge, this is one of the first studies to sequence and compare genetic alterations between patient-matched SCC primary tumors and lymph node metastases.

RESULTS

Primary metastatic tumors harbored a total of 41 mutations (18 pathogenic) or an average of 4.1 mutations per tumor. Nodal metastases harbored a total of 49 mutations (21 pathogenic) or an average of 4.9 mutations per tumor. All somatic mutations are summarized in Table 1. Several mutations had notable differences in mutational frequencies

[1]*Department of Dermatology, College of Medicine, University of Nebraska Medical Center, Omaha, Nebraska, USA;* [2]*Department of Dermatology, Keck School of Medicine of University of Southern California, University of Southern California, Los Angeles, California, USA; and* [3]*The Fred and Pamela Buffett Cancer Center, University of Nebraska Medical Center, Omaha, Nebraska, USA*

Correspondence: Ashley Wysong, Department of Dermatology, 985645 Nebraska Medical Center, Omaha, Nebraska 68198, USA. E-mail: ashley.wysong@unmc.edu

Abbreviations: ERK, extracellular signal−regulated kinase; SCC, squamous cell carcinoma

Received 20 September 2021; revised 11 February 2022; accepted 28 February 2022; accepted manuscript published online XXX; corrected proof published online XXX

Cite this article as: JID Innovations 2022;2:100122

Table 1. A Side-by-Side Summary of All Mutations for Primaries and Corresponding Metastases

Primary Tumor						Corresponding Metastasis					
ID	Gene	CDS	Protein	VAF	COSMIC	ID	Gene	CDS	Protein	VAF	COSMIC
						1M	*AKT3*	c.391G>A	p.E131K	0.30	P
						1M	*ALK*	c.3604_3605GG>AA	p.G1202K	0.29	NA
						1M	*ALK*	c.3605G>A	p.G1202E	0.27	P
1P	*CDKN2A*	c.253G>C	p.A85P	0.72	P						
						1M	*ERBB2*	c.2353C>T	p.L785F	0.29	P
						1M	*FAT1*	c.5013A>T	p.E1671D	0.29	NA
						1M	*FGFR3*	c.2156G>C	p.C719S	0.06	NA
						1M	*GNAQ*	c.554C>T	p.P185L	0.33	NA
1P	*HNF1A*	c.718G>A	p.E240K	0.50	P						
						1M	*JAK2*	c.2053G>A	p.E685K	0.22	NA
1P	*KDR*	c.934G>A	p.G312R	0.69	NA						
						1M	*MAP2K2*	c.189G>A	p.K63K	0.31	NA
						1M	*RB1*	c.1680C>T	p.S560S	0.35	NA
						1M	*STK11*	c.896C>T	p.S299F	0.26	P
1P	*TP53*	c.741_742CC>TT	p.R248W	0.61	NA						
						1M	*TP53*	c.915G>A	p.K305K	0.31	P
						1M	*TP53*	c.1027G>T	p.E343*	0.35	P

ID	Gene	CDS	Protein	VAF	COSMIC	ID	Gene	CDS	Protein	VAF	COSMIC
						2M	*ARID1A*	c.3940_3941CC>TT	p.P1314L	0.18	NA
						2M	*CDH1*	c.2243_2244CC>TT	p.T748I	0.40	NA
						2M	*CDKN2A*	c.172C>T	p.R58*	0.77	N
						2M	*GATA3*	c.895C>T	p.R299W	0.33	P
						2M	*HNF1A*	c.459C>T	p.P153P	0.27	NA
2P	*KDR*	c.3207G>A	p.L1069L	0.26	NA						
						2M	*KDR*	c.844_845GG>AA	p.G282K	0.43	NA
						2M	*NOTCH1*	c.1422C>T	p.F474F	0.33	NA
2P	*PTEN*	c.834C>G	p.F278L	0.79	P	2M	*PTEN*	c.834C>G	p.F278L	0.14	P
2P	*SMAD4*	c.1086T>C	p.F362F	1.60	NA	2M	*SMAD4*	c.1086T>C	p.F362F	0.77	NA
						2M	*TP53*	c.1006G>T	p.E336*	0.18	N
						2M	*TP53*	c.581delT	p.I195fs*52	0.45	NA

ID	Gene	CDS	Protein	VAF	COSMIC	ID	Gene	CDS	Protein	VAF	COSMIC
3P	*CDKN2A*	c.238C>T	p.R80*	0.24	P	3M	*CDKN2A*	c.238C>T	p.R80*	0.18	P
3P	*SMAD4*	c.1081C>T	p.R361C	0.29	P	3M	*SMAD4*	c.1081C>T	p.R361C	0.12	P
3P	*TP53*	c.535C>T	p.H179Y	0.23	P	3M	*TP53*	c.535C>T	p.H179Y	0.18	P
3P	*TP53*	c.372_374delin TA	p.C124Tfs	0.24	NA						

ID	Gene	CDS	Protein	VAF	COSMIC	ID	Gene	CDS	Protein	VAF	COSMIC
4P	*NOTCH1*	c.1393G>A	p.A465T	0.96	P	4M	*NOTCH1*	c.1393G>A	p.A465T	0.91	P
4P	*TP53*	c.499C>T	p.Q167*	0.94	P	4M	*TP53*	c.499C>T	p.Q167*	0.90	P

ID	Gene	CDS	Protein	VAF	COSMIC	ID	Gene	CDS	Protein	VAF	COSMIC
						5M	*ALK*	c.3567C>T	p.S1189S	0.42	NA
						5M	*ALK*	c.3644C>T	p.P1215L	0.44	NA
5P	*ARID1A*	c.2093_2094CC>TT delinsTT	p.S698F	0.40	NA						
5P	*CDKN2A*	c.323A>T	p.D108V	0.78	P						
5P	*ERBB2*	c.2336C>T	p.S779F	0.41	NA						
5P	*FGFR3*	c.817T>C	p.F273L	0.31	NA						
5P	*GNAS*	c.466G>C	p.D156H	0.29	NA						
5P	*HRAS*	c.38G>A	p.G13D	0.51	P						
5P	*KIT*	c.2458G>A	p.D820N	0.35	NA						
						5M	*NOTCH1*	c.1093C>T	p.R365C	0.43	P
5P	*PTEN*	c.864A>T	p.E288D	0.08	NA						
5P	*TP53*	c.265_266CC>TT	p.P89F	0.37	NA						
						5M	*TP53*	c.534_535CC>TT	p.H179Y	0.84	NA
5P	*TP53*	c.771_772GG>AA	p.E258K	0.46	NA						

ID	Gene	CDS	Protein	VAF	COSMIC	ID	Gene	CDS	Protein	VAF	COSMIC
6P	*FGFR2*	c.1651C>T	p.L551F	0.22	NA	6M	No mutations				
ID	**Gene**	**CDS**	**Protein**	**VAF**	**COSMIC**	**ID**	**Gene**	**CDS**	**Protein**	**VAF**	**COSMIC**
						7M	*CDH1*	c.2226_2227GC>CG	p.P743A	0.55	NA
7P	*FBXW7*	c.1209A>G	p.L403L	1.30	NA	7M	*FBXW7*	c.1209A>G	p.L403L	0.63	NA
7P	*TP53*	c.527G>A	p.C176Y	1.76	P	7M	*TP53*	c.527G>A	p.C176Y	0.47	P
ID	**Gene**	**CDS**	**Protein**	**VAF**	**COSMIC**	**ID**	**Gene**	**CDS**	**Protein**	**VAF**	**COSMIC**
8P	*APC*	c.3319_3335delCCAATGGTTCAGAAA	p.N1108_T1112del NGSET	0.29	NA						
8P	*CDH1*	c.2226_2227GC>CG	p.P743A	0.17	NA						
8P	*CDK4*	c.65A>T	p.K22M	0.42	P	8M	*CDK4*	c.65A>T	p.K22M	0.45	P
8P	*CDKN2A*	c.266G>T	p.G89V	0.92	P	8M	*CDKN2A*	c.266G>T	p.G89V	0.86	P
8P	*TP53*	c.824G>T	p.C275F	0.55	P	8M	*TP53*	c.824G>T	p.C275F	0.59	P
ID	**Gene**	**CDS**	**Protein**	**VAF**	**COSMIC**	**ID**	**Gene**	**CDS**	**Protein**	**VAF**	**COSMIC**
9P	*BAP1*	c.1454C>G	p.S485*	0.70	NA	9M	*BAP1*	c.1454C>G	p.S485*	0.69	NA
						9M	*DDR2*	c.2370C>T	p.S790S	0.31	NA
						9M	*EGFR*	c.848G>C	p.G283A	0.15	NA
9P	*ERBB3*	c.282C>T	p.F94F	0.43	NA	9M	*ERBB3*	c.282C>T	p.F94F	0.42	NA
9P	*KDR*	c.1481G>A	p.G494E	0.32	P	9M	*KDR*	c.1481G>A	p.G494E	0.33	P
9P	*KIT*	c.96G>A	p.G32G	0.38	NA	9M	*KIT*	c.96G>A	p.G32G	0.43	NA
9P	*SMO*	c.1203G>C	p.A401A	0.60	NA	9M	*SMO*	c.1203G>C	p.A401A	0.62	N
9P	*SMO*	c.1613C>T	p.T538I	0.41	NA	9M	*SMO*	c.1613C>T	p.T538I	0.47	NA
9P	*TP53*	c.574C>T	p.Q192*	0.42	P	9M	*TP53*	c.574C>T	p.Q192*	0.40	P
9P	*TP53*	c.586C>T	p.R196*	0.44	P	9M	*TP53*	c.586C>T	p.R196*	0.45	P
ID	**Gene**	**CDS**	**Protein**	**VAF**	**COSMIC**	**ID**	**Gene**	**CDS**	**Protein**	**VAF**	**COSMIC**
10P	*FBXW7*	c.1495G>T	p.G499C	0.34	NA	10M	None				
10P	*HRAS*	c.53C>T	p.A18V	0.30	P						

Abbreviations: ID, identification; CDS, coding sequence; delins, deletion insertion; N, neutral (COSMIC); NA, not reported in COSMIC; P, pathogenic (COSMIC); VAF, variant allele frequency (corrected for % tumor content)

between primary tumors versus metastases (Table 2). For the primary tumors, 68.3% (28 of 41) of mutations were missense, 14.3% (6 of 41) of mutations were silent, 11.9% (5 of 41) of mutations were nonsense, 2.4% (1 of 41) of mutations were frameshift, and 2.4% (1 of 41) of mutations were deletions. For metastases, 57.1% (28 of 49) of mutations were missense, 24.5% (12 of 49) of mutations were silent, 16.3% (8 of 49) of mutations were nonsense, and 2.0% (1 of 49) of mutations were frameshift. There were no statistically significant differences between primary tumors and metastases with respect to mutation type. For primary tumors, tumor suppressor gene was composed of 63.4% (26 of 41) of mutations and oncogenes were composed of 36.6% (15 of 41) of mutations. Metastases had a very similar distribution, with 61.2% (30 of 49) of mutations arising in tumor suppressor genes and 38.8% (19 of 49) of mutations arising in oncogenes.

The mutations with the greatest difference in frequency between primary tumors and metastases were *ALK* (four unique mutations in metastases and zero mutations in primary tumors), *HRAS* (present in 0% (0 of 10) of metastases and 20% (2 of 10) of primary tumors), and *NOTCH1* (present in 30% (3 of 10) of metastases and 10% (1 of 10) of primary tumors). Further analysis using Maftools/Oncodrive revealed *ALK* as a driver mutation in metastases (Figure 1) (Mayakonda et al., 2018; Tamborero et al., 2013). A second analysis was performed using R package dNdScv to evaluate the finding of *ALK* as a driver mutation. Using this package, *TP53*, *CDKN2A*, and *ALK* were all found to be significant driver mutations in metastatic SCC ($P < 0.001$, $P < 0.001$, and $P = 0.003$, respectively; Table 3) (Martincorena et al., 2017).

Mutation concordance was highly correlated to immune status. In immunosuppressed patients, 32.1% of mutations were concordant between primary tumors and metastases, whereas 54.9% of mutations in immunocompetent patients were concordant between primary tumors and metastases ($P = 0.04$). When only considering pathogenic mutations, this was even more apparent because 41.7% of mutations were concordant in immunosuppressed versus 83.3% of mutations in immunocompetent patients ($P = 0.01$). The mutational concordance of each gene is illustrated in Table 4. Mutations in *SMAD4*, *SMO*, *BAP1*, *CDK4*, and *ERBB3* were concordant between primary tumors and matched metastases 100% of the time (Table 4). Mutations in *TP53*, *FBXW7*, *KIT*, and *PTEN* were concordant in 66.7% of cases (Table 4). *NOTCH1* mutations were concordant 50% of the time, *KDR* mutations were concordant 40% of the time; and the remaining mutations were concordant in 0% of cases (Table 4).

Alexandrov et al. (2013) described over 20 mutational signatures in various human cancers that are described in COSMIC (Alexandrov et al., 2013; COSMIC, 2021). Because these are largely dependent on base pair changes, base pair

Table 2. A Summary of Mutations by Gene and the Differences between Primary Tumors and Metastases

Gene	Primary (n)	Metastases (n)	*P*-Value[1]
ALK	0	4	0.15
HRAS	2	0	0.15
NOTCH1	1	3	>0.05
TP53	10	11	>0.05
CDKN2A	4	3	>0.05
KDR	3	2	>0.05
FBXW7	2	1	>0.05
KIT	2	1	>0.05
PTEN	2	1	>0.05
CDH1	1	2	>0.05
APC	1	0	>0.05
FGFR2	1	0	>0.05
GNAS	1	0	>0.05
AKT3	0	1	>0.05
DDR2	0	1	>0.05
EGFR	0	1	>0.05
FAT1	0	1	>0.05
GATA3	0	1	>0.05
GNAQ	0	1	>0.05
JAK2	0	1	>0.05
MAP2K2	0	1	>0.05
RB1	0	1	>0.05
STK11	0	1	>0.05
SMAD4	2	2	>0.05
SMO	2	2	>0.05
ARID1A	1	1	>0.05
BAP1	1	1	>0.05
CDK4	1	1	>0.05
ERBB2	1	1	>0.05
ERBB3	1	1	>0.05
FGFR3	1	1	>0.05
HNF1A	1	1	>0.05

[1]Paired samples *t*-test; multiple mutations in one sample are counted as one.

Table 3. Significant Genes in our Cohort of SCC Lymph Node Metastases Identified in dNdScv

Gene	Global q-Value
TP53	<0.001
CDKN2A	<0.001
ALK	0.003

Abbreviation: SCC, squamous cell carcinoma

changes were analyzed in both groups and are illustrated in Figure 2a. Using the signature analysis module in Maftools, it was determined that the best match signature for primary tumors was Signature 5 (unknown etiology, previously described), and the best match for metastases was Signature 7 (UV exposure) (Figure 2b) (Lobl et al., 2020; Mayakonda et al., 2018).

DISCUSSION

Several mutations detected in our cohort are well established in SCC, including *TP53*, *NOTCH1*, and *CDKN2A* (Brown et al., 2004; Nagano et al., 1993; Wang et al., 2011). To our knowledge, this is the first report of *ALK* as a potential driver mutation in metastatic SCC. Oncogene *ALK* is a receptor protein-tyrosine kinase and member of the insulin receptor superfamily (Hallberg and Palmer, 2013; Iwahara et al., 1997). *ALK* mutations have been implicated in many human cancers, including non-small cell lung cancer, breast cancer, ovarian cancer, colorectal cancer, and renal cell carcinoma, among others (Hallberg and Palmer, 2013). The function of *ALK* has not been investigated in SCC with the exception of a recent study by Gualandi et al. (2020) that utilized a mouse model to show that *ALK* plays a role in the development of SCC (Gualandi et al., 2020). It was shown in mice that *Alk* exerts its tumorigenic role through cooperation with other well-known cancer-associated genes *Kras*, *Tp53*, and *Stat3* (Gualandi et al., 2020).

To understand the mechanism by which *ALK* may drive metastasis, we analyzed the context of each mutation and performed an additional analysis with R package TRONCO using the CAPRI program (De Sano et al., 2016). In the model created for SCC lymph node metastases, the *ALK* missense mutation conferred an evolutionary advantage to the tumor

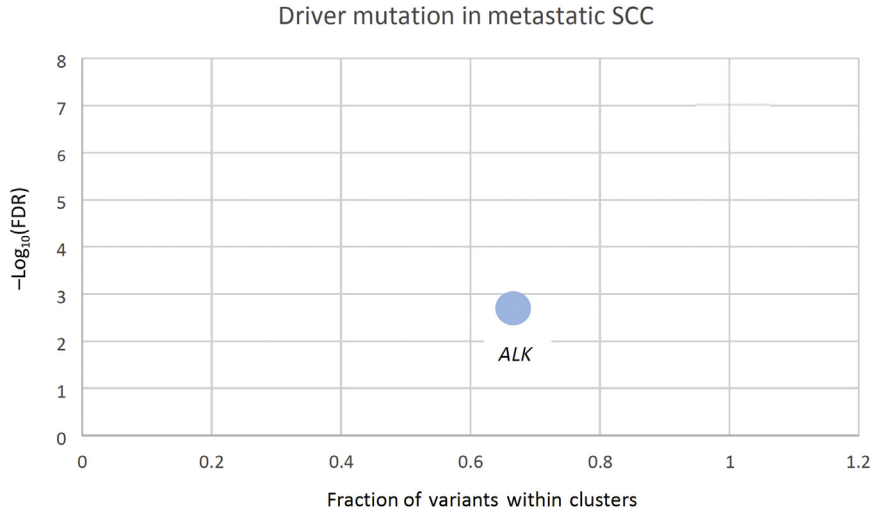

Figure 1. The driver mutation found in nodal metastases with the oncoCLUST algorithm. FDR, false discovery rate; SCC, squamous cell carcinoma.

Table 4. Rates of Mutational Concordance for All Genes Measured

Gene	Concordant (n)	Discordant (n)	Concordant Mutations (%)	Total # of Mutations	P or M
SMAD4	4	0	100	4	Both P and M
SMO	4	0	100	4	Both P and M
BAP1	2	0	100	2	Both P and M
CDK4	2	0	100	2	Both P and M
ERBB3	2	0	100	2	Both P and M
TP53	14	7	66.7	21	Both P and M
FBXW7	2	1	66.7	3	Both P and M
KIT	2	1	66.7	3	Both P and M
PTEN	2	1	66.7	3	Both P and M
CDKN2A	4	3	57.1	7	Both P and M
NOTCH1	2	2	50	4	Both P and M
KDR	2	3	40	5	Both P and M
ALK	0	4	0	4	M only
CDH1	0	3	0	3	Both P and M
ARID1A	0	2	0	2	Both P and M
ERBB2	0	2	0	2	Both P and M
FGFR3	0	2	0	2	Both P and M
HNF1A	0	2	0	2	Both P and M
HRAS	0	2	0	2	P Only
AKT3	0	1	0	1	M only
APC	0	1	0	1	P Only
DDR2	0	1	0	1	M only
EGFR	0	1	0	1	M only
FAT1	0	1	0	1	M only
FGFR2	0	1	0	1	P Only
GATA3	0	1	0	1	M only
GNAQ	0	1	0	1	M only
GNAS	0	1	0	1	P Only
JAK2	0	1	0	1	M only
MAP2K2	0	1	0	1	M only
RB1	0	1	0	1	M only
STK11	0	1	0	1	M only

Abbreviations: #, Number; M, metastasis; P, primary

that led to other downstream mutations in *FGFR3*, *JAK2*, *FAT1*, *ERBB2*, *TP53*, and *RB1* (Figure 3). Because *ALK, FGFR3, JAK2,* and *ERBB2* are all part of the RTK/RAS/MAPK pathway, these data led us to further look at mutations in this pathway. Future studies utilizing laser-capture microdissection and sampling from multiple sites to capture tumoral heterogeneity and representative variant allele frequencies would be an important next step to analyze tumor evolution.

In one patient, *ALK* and *ERBB2* were comutated in a metastasis (this *ERBB2* mutation was characterized as pathogenic in COSMIC); the other patient had an *ERBB2* mutation in the primary tumor and an *ALK* mutation in the metastasis. It is possible that *ALK* was also mutated in the primary tumor as a subclone below the 5% level threshold used to call variants in this study. *ALK* and *ERBB2* have been shown to act synergistically to promote tumor growth and survival in the studies using non-small cell lung cancer cell lines (Voena et al., 2013). A pathway analysis was performed to identify potential downstream targets of *ALK* and/or *ERBB2*. A common signaling pathway and possible mechanism for *ALK*-driven metastasis observed in this study is through the MAPK/extracellular signal–regulated kinase (ERK) signaling pathway. Hrustanovic and Bivona (2016) studied models of lung adenocarcinoma and determined that *ALK*-positive lung adenocarcinomas were dependent on the MAPK/ERK pathway for tumor survival. In addition, inhibition of this pathway along with *ALK* improved the magnitude and duration of response of *ALK*+ tumors in preclinical models (Hrustanovic and Bivona, 2016). A study using T-cell lymphoma cell lines determined that *ALK* fusion activates MAPK/ERK kinase 1/2 and ERK1/2 (Marzec et al., 2007). *ERBB2* is upstream activator of the MAPK/ERK pathway (Feng et al., 2018). The MAPK/ERK pathway has been shown to play a role in metastasis for several cancers (Li et al., 2020; Yan et al., 2018). We hypothesize that *ALK* mutations, possibly in combination with *ERBB2*, activate the MAPK/ERK pathway, ultimately leading to growth, survival, and metastasis of SCCs.

A study by Li et al. (2015) performed targeted sequencing on 29 SCC lymph node metastases and found that 27.6% (8 of 29) of samples had an *ALK* mutation, which is similar to our study in which 20% (2 of 10) of patients harbored an *ALK* mutation (4 unique mutations). Li et al. (2015) also detected *ERBB2* mutations in 20.7% (6 of 29) of patients, 50% (3 of 6)

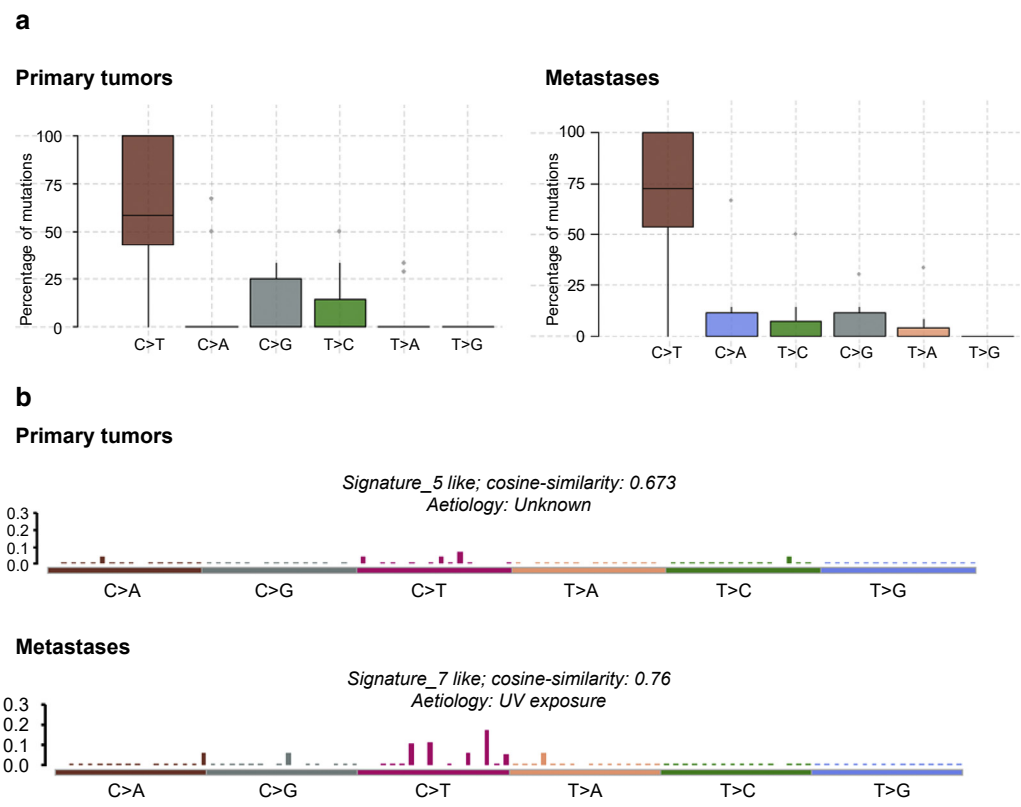

Figure 2. Distribution of mutations (a) and COSMIC signatures (b) in primary tumors and metastases.

of which co-occurred with *ALK* mutations. Running Maftools program SomaticInteractions on this data revealed that *ERBB2* and *ALK* mutations have an OR of co-occurrence of 5.3. However, this only leans toward statistical significance, which may be due to the relatively small sample size of 29 patients ($P = 0.16$) (Li et al., 2015; Mayakonda et al., 2018).

A literature review of *ALK* mutations in localized SCCs shows mutations in 10–25% of localized tumors (Durinck et al., 2011; Feng et al., 2018; Inman et al., 2018). Because *ALK* is mutated in many human cancers, there are Food and Drug Administration-approved and developing therapeutics (crizotinib, ceritinib, and others) that target *ALK* mutations and have improved patient outcomes by blocking angiogenesis and metastasis (Hallberg and Palmer, 2013; Kwak et al., 2010; Shaw et al., 2014). *ALK* may be a potential therapeutic target for adjuvant therapy of high-risk locally advanced SCCs and treatment of metastatic disease. If further studies support a synergistic role of *ERBB2* and *ALK* in SCC growth and metastasis, inhibitors of *ERBB2* such as afatinib can be used clinically in *ERBB2*-mutated cancers and may be effective in preventing *ALK*-inhibitor resistance (Tanizaki et al., 2012).

Although *ALK* may act as a driver in SCC, alternative interpretations of the data must be considered. One observation that should be investigated in future studies is that *ALK* mutations were present in lymph node metastases and not primary tumors. There are several possibilities for these findings. It is possible that *ALK* was also mutated in the primary tumor as a subclone below the 5% level threshold used

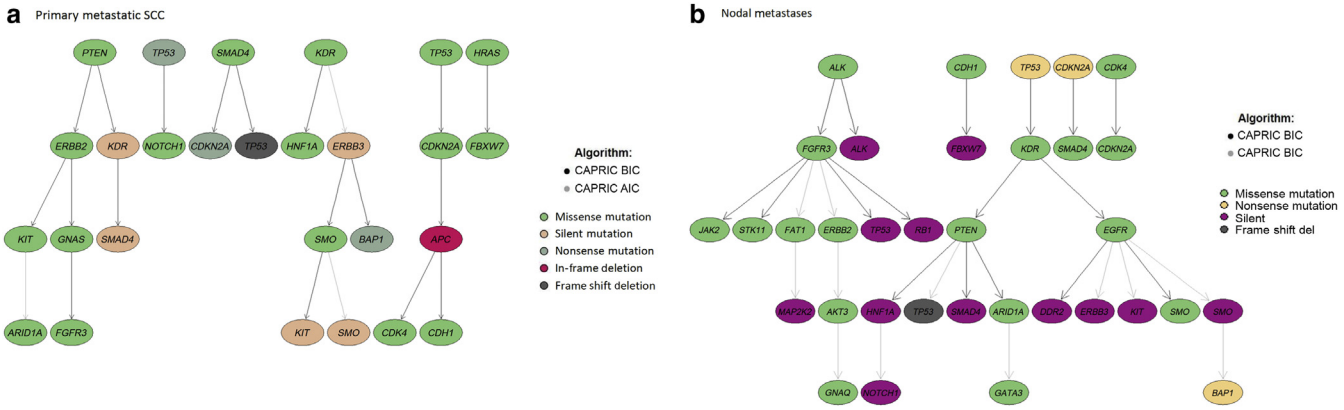

Figure 3. Hypothesis of mutational progression in SCC. AIC, Akaike Information Criteria; BIC, Bayesian information Criteria; SCC, squamous cell carcinoma.

to call variants in this study. Another possibility is that *ALK* mutations are acquired later in the metastatic process and therefore are not actually necessary for the initiation of the process but drives the more advanced metastatic process. Alternatively, it is possible that *ALK* is not necessary to drive SCC metastases and a pathogenic variant was acquired that acted more like a passenger mutation. Future studies with larger sample sizes examining *ALK* as a driver mutation may help to answer this research question.

Performing sequencing on both primary tumors and metastases and considering the optimal time for intervention may be important when selecting patients for targeted therapies, which includes EGFR inhibitor cetuximab (Trodello et al., 2019, 2017). Although cetuximab has shown some clinical benefit in treating SCC, EGFR tyrosine kinase inhibitors gefitinib and erlotinib have shown little efficacy in clinical trials (Gold et al., 2018; William et al., 2017). However, augmenting EGFR tyrosine kinase inhibitor therapy with topical ointment of miR-634 has shown promising effect in preclinical studies (Inoue et al., 2020). One study by Yilmaz et al. (2017) performed whole exome sequencing on SCCs that included six pairs of matched primary tumors and metastases. An overall concordance rate of 70.8% was found when looking at a subset of 26 genes previously determined to be mutated in SCC (34 concordant mutations and 14 discordant mutations) (Yilmaz et al., 2017). This rate is very similar to the concordance rate for pathogenic mutations in our cohort (66.7% concordance). In our study, mutations in *SMAD4, SMO, BAP1, CDK4,* and *ERBB3* were concordant between primary tumors and metastases in 100% of cases, suggesting that these mutations likely occur early and may be consistent throughout the tumor progression. *CDK4* was previously shown to have positive expression in 53.3% (16 of 30) of SCCs (Lu et al., 1999). *CDK4* may be a potential therapeutic target in SCC as CDK4/6 inhibitor abemaciclib has shown benefit for metastatic breast cancer patients and is in many clinical trials for other metastatic cancers (Dickler et al., 2017).

To the best of our knowledge, this is the first study to examine the effect of immune status on mutational concordance between SCC primary tumors and metastases. A study of breast cancer matched primary tumors and metastases, examined immune cells in the tumor microenvironment of primary and metastases, and found notable differences, particularly with respect to PD-L1 expression (Cimino-Mathews et al., 2016). We hypothesize that the tumor microenvironment has a greater impact on tumor progression in immunosuppressed patients, resulting in a lower proportion of concordant mutations in immunosuppressed patients. Clinically, this is especially relevant when selecting adjuvant therapies to treat both primary tumors and metastases. For example, sequencing is typically done on the primary tumor, and the genes mutated in the primary are targeted by selected systemic therapies. However, the primary tumor is often excised surgically, leaving the metastases to be treated with systemic therapy. Given the substantial lack of mutational concordance between primary tumors and metastases, especially in immunosuppressed patients, sequencing of the metastases may be considered when identifying patient–specific adjuvant therapies.

Mutational processes in cancer generate unique combinations of mutations types, termed mutational signatures. Our data show that C>T mutations comprise a majority of total mutations in high-risk SCC and that COSMIC Signature 7 is the best fit for metastases. Signature 7 is associated with large numbers of CC>TT mutations at dipyrimidines that are typically repaired by nucleotide excision repair (Alexandrov et al., 2013). Mueller et al. (2019) performed whole genome sequencing on 15 SCC metastases (six parotid and nine neck lymph node) and found Signature 7 to correlate best with the somatic mutations. The clinical utility of these mutational signatures was suggested by Mueller et al. (2019) because the UV signatures were able to differentiate metastases of mucosal origin from metastases of cutaneous origin. In addition, Signature 7 may be helpful in prognosis and helping to identify a more high-risk subset of SCC.

Overall, we present results from a targeted next-generation sequencing study of 10 primary metastatic SCCs that were patient–matched with 10 lymph node metastases. We report *ALK* as a potential driver mutation for metastases in SCC. *ALK* mutations were observed to co-occur with *ERBB2* mutations in our cohort, suggesting a possible mechanism for *ALK*-driven metastasis is through the MAPK/ERK signaling pathway. In addition, we found that mutational concordance between primary and metastatic tumor was significantly lower in immunosuppressed patients. Because these findings may have clinical implications, validation studies and evaluation of gene expression and pathways in metastatic SCC would be beneficial.

The limitations of this sequencing study include that it was performed using one sample of tissue per primary tumor or metastasis at a single time point. Mutations detected in metastases but not in the matched primary tumor may have been acquired throughout tumorigenesis, developed from a subclone not captured in tumor sampling, or passenger mutations not essential for clonal expansion and initial spread (Guillermin et al., 2018). One particular limitation of using a single sample of tissue per tumor is that intratumoral heterogeneity is not able to be captured in the analysis. Because heterogeneity has been shown to play an important role in tumor pathogenesis, future studies that analyze multiple samples per tumor would be of particular value.

Targeted sequencing studies have several limitations and benefits. Although it is cost effective and the depth of coverage and sensitivity is greater than that would be possible with whole-exome or whole-genome sequencing, the amount of DNA sequenced is much smaller and only reflects specific genes targeted by a specific panel. It is possible that a targeted sequencing study may miss important mutations that are not included in the specific panel. An additional limitation to this study was our limited sample size. Additional studies with larger sample sizes would be helpful as a validation cohort.

MATERIALS AND METHODS

All human studies were approved by the authors' Institutional Review Board (University of Southern California, Los Angeles, CA; number HS-17-00397) and each subject provided informed written consent. A cohort of 10 patients was developed for this study (Table 5). Inclusion criteria were patients presenting to our academic medical center between 2014 and 2017 with histologically confirmed metastatic SCC. All patients had both primary tumor and

Table 5. A Summary of the Cohort Characteristics

Patient and Tumor Characteristics	Count and Averages
Average age (y)	68.1
Males/females	8/2
Location	Primary tumors:
	Ear (5)
	Nose (1)
	Scalp (3)
	Supraorbital (1)
	Metastases: Lymph node (10)
BWH stage	T1 (1)
	T2a (3)
	T2b (2)
	T3 (4)
Immune status	Immunocompetent (6)
	Immunosuppressed (4)

Abbreviations: BWH, XXX

metastatic tumor tissue available for analysis. Exclusion criteria were patients without histologically confirmed metastasis and patients with noncutaneous SCCs. The Vela OncoKey Select Panel (with 76 cancer-associated genes) was run on formalin-fixed paraffin-embedded samples. One reason for the selection is that this gene panel targets genes specifically known to be mutated in many human cancers. Another reason for selecting the panel and the targeted sequencing approach is that it provides a higher sensitivity for cancer specific genes than a broader panel or a whole genome or whole exome sequencing approach. The median coverage of this assay is greater than ×500. The coverage of each specific gene is detailed in Table 6. H&E-stained sections were evaluated by board-certified pathologists to determine percent tumor content in areas selected for DNA extraction. Macrodissections were made on unstained tissue sections, and genomic DNA was isolated using the Maxwell FFPE DNA ISOlation Kit (Promega, Madison, WI). This was used to calculate the corrected variant allele frequency for each mutation. A cutoff of variant allele frequency of 0.05 was used to call mutations (uncorrected). Additional details regarding the sequencing, alignment, coverage parameters, and analysis are detailed in the user manual (available at veladx.com). Classification of variants was performed using published literature and public databases such as dbSNP (https://www.ncbi.nlm.nih.gov/snp/), ClinVar (https://www.ncbi.nlm.nih.gov/clinvar/), and COSMIC (https://cancer.sanger.ac.uk/cosmic) (ClinVar, 2021; COSMIC, 2021; Sherry et al., 1999).

Statistical analyses were performed with R Studio version 3.6.1 and Excel version 16.35 (Microsoft, Redmond, WA). Within the R Maftools package, various functions were used for data analysis: TiTv to calculate the distribution of base pair changes; trinucleotideMatrix, extractSignatures, and plotSignatures to obtain and visualize mutational signatures; and Oncodrive to identify driver mutations (Mayakonda et al., 2018; Tamborero et al., 2013). Alexandrov et al. (2013) described over 20 mutational signatures in various human cancers. Using the signature analysis module in Maftools, mutational signatures were computed for our cohort and compared to previously described signatures using cophenetic correlation and non-negative matrix factorization. Cosine similarity is used to identify the signature(s) that are the best match(es) for the input data. Additional R packages used for analyses include

Table 6. Panel Coverage of Each Gene From veladx.com

Genes	No. of Amplicons	Exons
AKT1	1	4
AKT2	1	3
AKT3	3	3, 5, 6
ALK	7	20, 22, 23, 24, 25
APC	10	16
AR	2	5, 8
ARAF	1	7
ARID1A	9	5, 8, 14, 15, 16, 18, 20
BAP1	8	4, 7, 9, 10, 12, 13, 16
BRAF	3	11, 15
BRCA1	2	3, 10
BRCA2	2	11, 27
CDH1	4	2, 3, 6, 14
CDK4	1	2
CDKN2A	3	1, 2
CSF1R	2	7, 22
CTCF	8	3, 4, 5, 6, 7, 8, 10
CTNNB1	1	3
DDR2	1	18
EGFR	8	3, 7, 15, 18, 19, 20, 21
ERBB2	8	8, 17, 18, 19, 20, 21, 22, 24
ERBB3	6	2, 3, 6, 7, 8
ERBB4	5	1, 3, 18, 21, 25
ESR1	4	6, 7, 9, 10
FAT1	2	10, 15
FBXW7	10	4, 5, 7, 8, 9, 10, 11, 12
FGFR1	5	4, 7, 12, 14, 15
FGFR2	6	3, 7, 9, 12, 14
FGFR3	5	7, 9, 14, 16, 18
FOXL2	1	1
GATA3	2	4, 6
GNA11	2	4, 5
GNAQ	2	4, 5
GNAS	4	6, 8, 9, 11
H3F3A	1	1
HIST1H3B	1	1
HNF1A	9	1, 2, 3, 4
HRAS	4	2, 3, 4
IDH1	1	4
IDH2	2	4
JAK2	3	12, 14, 16
KDR	10	7, 8, 11, 15, 22, 23, 24
KEAP1	1	4
KIT	15	2, 8, 9, 10, 11, 12, 13, 14, 17, 18
KMT2C	2	15, 34
KMT2D	4	32, 33, 48, 53
KRAS	3	2, 3, 4
MAP2K1	7	2, 3, 4, 6, 7, 11
MAP2K2	1	2
MAP3K1	3	4, 14, 17
MET	7	13, 14, 16, 19, 20
MLH1	1	12
MTOR	4	24, 39, 47, 53
NF1	4	9, 12, 35, 50
NFE2L2	2	2
NOTCH1	8	6, 8, 26, 27, 34
NRAS	4	2, 3, 4

(*continued*)

Table 6. Continued

Genes	No. of Amplicons	Exons
PDGFRA	4	12, 14, 18
PIK3CA	11	2, 5, 8, 10, 14, 21
PIK3R1	8	9, 10, 11, 12, 13, 14, 15
POLE	2	9, 13
PTEN	23	1, 2, 3, 4, 5, 6, 7, 8, 9
RAC1	3	2, 5, 6
RB1	5	10, 11, 14, 17, 20
RET	7	10, 11, 13, 15, 16
RHOA	3	2, 3
ROS1	2	36, 38
SF3B1	5	14, 15, 16, 18
SMAD4	7	3, 9, 10, 11, 12
SMARCB1	4	2, 4, 5, 9
SMO	4	3, 6, 8, 9
SRC	1	13
STK11	22	1, 2, 3, 4, 5, 6, 7, 8, 9
TP53	23	2, 3, 4, 5, 6, 7, 8, 9, 10, 11
TSC1	1	15
TSC2	2	17, 30
U2AF1	2	2, 6
VHL	3	1, 2, 3

Abbreviations: No., number

TRONCO and dNdScv (De Sano et al., 2016; Martincorena et al., 2017). Within TRONCO, the CAPRI function was used. CAPRI takes results from mutation studies and constructs a proposed model of tumor evolution based on The Cancer Genome Atlas data and previous sequencing studies (De Sano et al., 2016). dNdScv works to detect driver mutations through quantification of selection in cancer by maximum-likelihood dN/dS methods (Martincorena et al., 2017). In a separate analysis, mutational concordance rates between primary and metastatic samples were calculated by counting the number of mutations that were seen in both matched primary and metastatic samples (concordant mutations), dividing this number by the total of all concordant and discordant mutations, and multiplying by 100.

Data availability statement

Datasets related to this article can be found at the following links hosted by National Center for Biotechnology Information Gene Expression Omnibus: GSE150727 (for primary metastatic tumors) https://www.ncbi.nlm.nih.gov/geo/query/acc.cgi?acc=GSE150727 and GSE196601 (for lymph node metastases) https://www.ncbi.nlm.nih.gov/geo/query/acc.cgi?acc=GSE196601.

ORCIDs

Marissa B. Lobl: http://orcid.org/0000-0002-8128-613X
Dillon D. Clarey: http://orcid.org/0000-0003-1076-2781
Shauna Higgins: http://orcid.org/0000-0002-1190-7033
Adam Sutton: http://orcid.org/0000-0002-1365-4703
Ashley Wysong: http://orcid.org/0000-0001-5131-1149

AUTHOR CONTRIBUTIONS

Conceptualization: AW, AS; Data Curation: AW, SH, MBL; Formal Analysis: AW, MBL; Supervision: AW, AS; Writing - Original Draft Preparation: MBL; Writing - Review and Editing: AW, AS, SH, DDC, MBL

CONFLICT OF INTEREST

AW serves as a Research Principal Investigator for Castle Biosciences. The remaining authors state no conflict of interest.

ACKNOWLEDGMENTS

We would like to acknowledge Pamela Ward, Mihaela Campan, and Rupali Arora for their help preparing the samples for sequencing. We would like to thank the Wright Foundation for their generous funding for this study.

REFERENCES

Alexandrov LB, Nik-Zainal S, Wedge DC, Aparicio SAJR, Behjati S, Biankin AV, et al. Signatures of mutational processes in human cancer [published correction appears in Nature 2013;502:258]. Nature 2013;500:415–21.

Al-Rohil RN, Tarasen AJ, Carlson JA, Wang K, Johnson A, Yelensky R, et al. Evaluation of 122 advanced-stage cutaneous squamous cell carcinomas by comprehensive genomic profiling opens the door for new routes to targeted therapies. Cancer 2016;122:249–57.

American Cancer Society. Information and Resources about for Cancer: Breast. Colon, lung, prostate, skin. 2018. https://www.cancer.org/content/dam/cancerorg/research/cancer-facts-and-statistics/annual-cancer-facts-and-figures/2018/cancer-facts-and-figures2018. (accessed May 1, 2020).

Bernal Martínez ÁJ, Fernández Letamendi N, Delgado Martínez J, Sampietro de Luis JM, Gómez-Escolar Larrañaga L, Sanz Aranda E. Risk factors and mortality in cutaneous squamous cell carcinoma of the head and neck. Actas Dermosifiliogr (Engl Ed) 2020;111:325–8.

Brougham NDLS, Dennett ER, Cameron R, Tan ST. The incidence of metastasis from cutaneous squamous cell carcinoma and the impact of its risk factors. J Surg Oncol 2012;106:811–5.

Brown VL, Harwood CA, Crook T, Cronin JG, Kelsell DP, Proby CM. p16INK4a and p14ARF tumor suppressor genes are commonly inactivated in cutaneous squamous cell carcinoma. J Invest Dermatol 2004;122:1284–92.

Cimino-Mathews A, Thompson E, Taube JM, Ye X, Lu Y, Meeker A, et al. PD-L1 (B7-H1) expression and the immune tumor microenvironment in primary and metastatic breast carcinomas. Hum Pathol 2016;47:52–63.

ClinVar. https://www.ncbi.nlm.nih.gov/clinvar/; 2021. (accessed May 30, 2021).

COSMIC. Catalogue of Somatic Mutations in Cancer. 2021. https://cancer.sanger.ac.uk/cosmic. (accessed April 16, 2021).

De Sano L, Caravagna G, Ramazzotti D, Graudenzi A, Mauri G, Mishra B, et al. TRONCO: an R package for the inference of cancer progression models from heterogeneous genomic data. Bioinformatics 2016;32:1911–3.

Dickler MN, Tolaney SM, Rugo HS, Cortés J, Diéras V, Patt D, et al. MONARCH 1, a phase II study of abemaciclib, a CDK4 and CDK6 inhibitor, as a single agent, in patients with refractory HR^{+}/$HER2^{-}$ metastatic breast cancer [published correction appears in Clin Cancer Res 2018;24:5485]. Clin Cancer Res 2017;23:5218–24.

Durinck S, Ho C, Wang NJ, Liao W, Jakkula LR, Collisson EA, et al. Temporal dissection of tumorigenesis in primary cancers. Cancer Discov 2011;1:137–43.

Feng Y, Spezia M, Huang S, Yuan C, Zeng Z, Zhang L, et al. Breast cancer development and progression: risk factors, cancer stem cells, signaling pathways, genomics, and molecular pathogenesis. Genes Dis 2018;5:77–106.

Genders RE, Weijns ME, Dekkers OM, Plasmeijer EI. Metastasis of cutaneous squamous cell carcinoma in organ transplant recipients and the immunocompetent population: is there a difference? a systematic review and meta-analysis. J Eur Acad Dermatol Venereol 2019;33:828–41.

Gold KA, Kies MS, William WN Jr, Johnson FM, Lee JJ, Glisson BS. Erlotinib in the treatment of recurrent or metastatic cutaneous squamous cell carcinoma: a single-arm phase 2 clinical trial. Cancer 2018;124:2169–73.

Gualandi M, Iorio M, Engeler O, Serra-Roma A, Gasparre G, Schulte JH, et al. Oncogenic ALK^{F1174L} drives tumorigenesis in cutaneous squamous cell carcinoma. Life Sci Alliance 2020;3:e201900601.

Guillermin Y, Lopez J, Chabane K, Hayette S, Bardel C, Salles G, et al. What does this mutation mean? The tools and pitfalls of variant interpretation in lymphoid malignancies. Int J Mol Sci 2018;19:1251.

Hallberg B, Palmer RH. Mechanistic insight into ALK receptor tyrosine kinase in human cancer biology [published correction appears in Nat rev Cancer 2013;13:820]. Nat Rev Cancer 2013;13:685–700.

Hrustanovic G, Bivona TG. RAS signaling in ALK fusion lung cancer. Small GTPases 2016;7:32–3.

Inman GJ, Wang J, Nagano A, Alexandrov LB, Purdie KJ, Taylor RG, et al. The genomic landscape of cutaneous SCC reveals drivers and a novel azathioprine associated mutational signature. Nat Commun 2018;9:3667.

Inoue J, Fujiwara K, Hamamoto H, Kobayashi K, Inazawa J. Improving the efficacy of EGFR inhibitors by topical treatment of cutaneous squamous cell carcinoma with miR-634 ointment. Mol Ther Oncolytics 2020;19:294–307.

Iwahara T, Fujimoto J, Wen D, Cupples R, Bucay N, Arakawa T, et al. Molecular characterization of ALK, a receptor tyrosine kinase expressed specifically in the nervous system. Oncogene 1997;14:439–49.

Joseph MG, Zulueta WP, Kennedy PJ. Squamous cell carcinoma of the skin of the trunk and limbs: the incidence of metastases and their outcome. Aust N Z J Surg 1992;62:697–701.

Karia PS, Han J, Schmults CD. Cutaneous squamous cell carcinoma: estimated incidence of disease, nodal metastasis, and deaths from disease in the United States, 2012. J Am Acad Dermatol 2013;68:957–66.

Kwak EL, Bang YJ, Camidge DR, Shaw AT, Solomon B, Maki RG, et al. Anaplastic lymphoma kinase inhibition in non-small-cell lung cancer [published correction appears in N Engl J Med 2011;364:588]. N Engl J Med 2010;363:1693–703.

Li QT, Feng YM, Ke ZH, Qiu MJ, He XX, Wang MM, et al. KCNN4 promotes invasion and metastasis through the MAPK/ERK pathway in hepatocellular carcinoma. J Investig Med 2020;68:68–74.

Li YY, Hanna GJ, Laga AC, Haddad RI, Lorch JH, Hammerman PS. Genomic analysis of metastatic cutaneous squamous cell carcinoma. Clin Cancer Res 2015;21:1447–56.

Lindelöf B, Sigurgeirsson B, Gäbel H, Stern RS. Incidence of skin cancer in 5356 patients following organ transplantation. Br J Dermatol 2000;143:513–9.

Lobl MB, Clarey D, Higgins S, Sutton A, Hansen L, Wysong A. Targeted next-generation sequencing of matched localized and metastatic primary high-risk SCCs identifies driver and co-occurring mutations and novel therapeutic targets. J Dermatol Sci 2020;99:30–43.

Lu Q, Lu F, Yang Z, Wen H, Yan L, Chen S, et al. Study on regulators of the cell cycle in cutaneous squamous cell carcinoma. Hunan Yi Ke Da Xue Xue Bao 1999;24:438–40.

Mansouri B, Housewright CD. The treatment of actinic keratoses - the rule rather than the exception. JAMA Dermatol 2017;153:1200.

Martincorena I, Raine KM, Gerstung M, Dawson KJ, Haase K, Van Loo P, et al. Universal patterns of selection in cancer and somatic tissues [published correction appears in Cell 2018;173:1823]. Cell 2017;171:1029–41.e21.

Marzec M, Kasprzycka M, Liu X, Raghunath PN, Wlodarski P, Wasik MA. Oncogenic tyrosine kinase NPM/ALK induces activation of the MEK/ERK signaling pathway independently of c-Raf. Oncogene 2007;26:813–21.

Mayakonda A, Lin DC, Assenov Y, Plass C, Koeffler HP. Maftools: efficient and comprehensive analysis of somatic variants in cancer. Genome Res 2018;28:1747–56.

Mueller SA, Gauthier MA, Ashford B, Gupta R, Gayevskiy V, Ch'ng S, et al. Mutational patterns in metastatic cutaneous squamous cell carcinoma. J Invest Dermatol 2019;139:1449–58.e1.

Nagano T, Ueda M, Ichihashi M. Expression of p53 protein is an early event in ultraviolet light-induced cutaneous squamous cell carcinogenesis. Arch Dermatol 1993;129:1157–61.

Rogers HW, Weinstock MA, Feldman SR, Coldiron BM. Incidence estimate of nonmelanoma skin cancer (keratinocyte carcinomas) in the U.S. population, 2012. JAMA Dermatol 2015;151:1081–6.

Shaw AT, Kim DW, Mehra R, Tan DSW, Felip E, Chow LQM, et al. Ceritinib in ALK-rearranged non-small-cell lung cancer. N Engl J Med 2014;370:1189–97.

Sherry ST, Ward M, Sirotkin K. dbSNP-database for single nucleotide polymorphisms and other classes of minor genetic variation. Genome Res 1999;9:677–9.

Tamborero D, Gonzalez-Perez A, Lopez-Bigas N. OncodriveCLUST: exploiting the positional clustering of somatic mutations to identify cancer genes. Bioinformatics 2013;29:2238–44.

Tanizaki J, Okamoto I, Okabe T, Sakai K, Tanaka K, Hayashi H, et al. Activation of HER family signaling as a mechanism of acquired resistance to ALK inhibitors in EML4-ALK-positive non-small cell lung cancer. Clin Cancer Res 2012;18:6219–26.

Trodello C, Higgins S, Ahadiat O, Ragab O, In G, Hawkins M, et al. Cetuximab as a component of multimodality treatment of high-risk cutaneous squamous cell carcinoma: a retrospective analysis from a single tertiary Academic Medical Center. Dermatol Surg 2019;45:254–67.

Trodello C, Pepper JP, Wong M, Wysong A. Cisplatin and cetuximab treatment for metastatic cutaneous squamous cell carcinoma: a systematic review. Dermatol Surg 2017;43:40–9.

Voena C, di Giacomo F, Panizza E, D'Amico L, Boccalatte FE, Pellegrino E, et al. The EGFR family members sustain the neoplastic phenotype of ALK+ lung adenocarcinoma via EGR1. Oncogenesis 2013;2:e43.

Wang NJ, Sanborn Z, Arnett KL, Bayston LJ, Liao W, Proby CM, et al. Loss-of-function mutations in Notch receptors in cutaneous and lung squamous cell carcinoma. Proc Natl Acad Sci USA 2011;108:17761–6.

William WN Jr, Feng L, Ferrarotto R, Ginsberg L, Kies M, Lippman S, et al. Gefitinib for patients with incurable cutaneous squamous cell carcinoma: a single-arm phase II clinical trial. J Am Acad Dermatol 2017;77:1110–3.e2.

Yan P, Zhu H, Yin L, Wang L, Xie P, Ye J, et al. Integrin αvβ6 promotes lung cancer proliferation and metastasis through upregulation of IL-8–mediated MAPK/ERK signaling. Transl Oncol 2018;11:619–27.

Yilmaz AS, Ozer HG, Gillespie JL, Allain DC, Bernhardt MN, Furlan KC, et al. Differential mutation frequencies in metastatic cutaneous squamous cell carcinomas versus primary tumors. Cancer 2017;123:1184–93.